Privileged structures: synthesis and structural investigations on tricyclic sulfonamides†

Maria Altamura,[a] Valentina Fedi,[a] Danilo Giannotti,[a] Paola Paoli*[b] and Patrizia Rossi[b]

Received (in Gainesville, FL, USA) 22nd June 2009, Accepted 4th August 2009
First published as an Advance Article on the web 1st September 2009
DOI: 10.1039/b9nj00279k

Customized synthetic procedures for the obtainment of highly functionalizable free sulfonamide tricyclic structures having NH, O, S and SO_2 (Z group) in the central seven-membered ring are presented. Due to the role that tricycles and the sulfonamide group play in medicinal chemistry, attention have been also paid to the 3D arrangement of these molecules. Their molecular structures and conformational properties have been studied by single-crystal X-ray diffraction and quantum chemical methods (HF-SCF/6-311 + G(d,p). The minimum energy geometries in the solid state (**I**, Z = O; **II**, Z = NH and **III**, Z = S, SO_2) have been compared with the minimum-energy geometries in the gas phase (invariably the type **III** geometry) and discussed with respect to the literature reference values. An effort was made to correlate the conformational differences observed in the solid-state and gas-phase with the nature of the Z grouping.

Introduction

The definition of the so-called "privileged structures" dates by now twenty years.[1] Amongst the molecular moieties recognized as being able to provide high affinity ligands for many types of receptors, tricycles (Fig. 1) play an important role both in the field of the drugs for the central nervous system and in other very different applications as reported recently.[2] It is easy to single out tricyclic structures of the general formula depicted in Fig. 1, either in anticancer agents such as farnesyl protein transferase agents, or in multidrug resistance modulators, HDAC inhibitors,[3] antiviral agents such as the non nucleoside inhibitors of HIV reverse transcriptase, antihistaminic drugs as loratadine or cyproheptadine.[2]

Amongst these structures, our research group has developed over the past years a particular interest for the skeletons containing an amide (**A**) or a sulfonamide function (**B**) (Fig. 2).[3,4]

While many general methods of synthesis are available for the skeleton containing the amide function in the central ring (**A**),[5] only a few focused examples are described for the synthesis of the analogs containing the free sulfonamide function (**B**).[6] The lack of a good, general and reproducible method of synthesis for these structures could have prevented their use in a larger number of applications. Despite this, the sulfonamide skeletons possess some peculiar properties in terms of both chemical and pharmacological versatility since they contain positions which are functionalizable in different conditions. In particular the strongly acidic, easily extractable, SO_2NH hydrogen represents an easy access to the post functionalization, and the activation to the substitution of some aromatic positions operated by the sulfonamide function renders these molecules an ideal platform for new derivatives.

In the present work we describe general methods for the obtainment of highly functionalizable free sulfonamide tricyclic structures (**B**), containing respectively NH, O, S and SO_2 in the central seven-membered ring. The unsubstituted dibenzodithiazepine 5,5-dioxide structure (Fig. 2, Z = S) and its oxidized product (Fig. 2, Z = SO_2) are described here for the first time and complete the series represented in Fig. 2. In addition a structural investigation of all the monomers sketched in Fig. 3 by both experimental (by single-crystal X-ray diffraction) and theoretical (by quantum chemical calculations) approaches is also presented. In particular, attention has been focused on the conformation of the sulfonamide moiety and the present experimental data and what is considered the standard conformation in sulfonamides are compared and discussed. In fact, given that several bio logically important compounds feature this functional group,[7] we think that the comprehension of the conformational

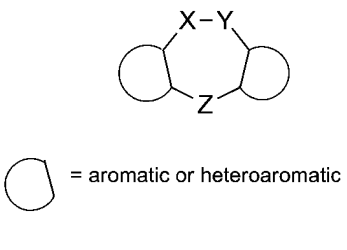

Fig. 1 Schematic drawing of a tricyclic skeleton.

[a] *Chemistry Department, Menarini Ricerche S.p.A., Florence, Italy*
[b] *Department of Energy Engineering "Sergio Stecco", University of Florence, Italy. E-mail: paolapaoli@unifi.it*

† Electronic supplementary information (ESI) available: Crystal packing of compounds. Tables S1–S6: Intermolecular hydrogen bonds and π–π interactions in the crystal lattices; most relevant geometrical parameters of the theoretically calculated structures. Scheme S1: Schematic representation of the intermolecular interactions in the compounds. CCDC reference numbers 745476–745481. For ESI and crystallographic data in CIF or other electronic format see DOI: 10.1039/b9nj00279k

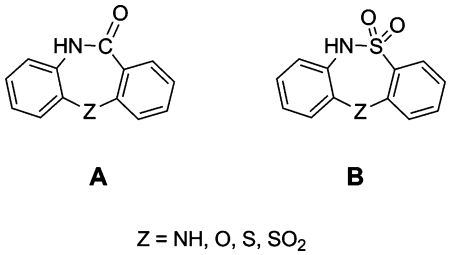

Fig. 2 Examples of tricyclic structures featuring amide and sulfonamide functionalities.

behaviour of this functionality is one of the key steps in order to clarify the way these species act at the molecular level.[8]

In addition the solid-state crystal structures of some of the dimers as obtained by single-crystal X-ray diffraction analysis is also presented.

Results and discussion

Synthesis

The few synthetic methods described in the literature for the synthesis of sulfonamides (**B**) usually refer to the condensation of phenylenediamines or 2-aminophenols with 2-chlorobenzenesulfonyl chlorides, where the halogen is easily substituted due to the presence of a strong activator in position 5 such as NO_2 (Scheme 1).[6] Otherwise some examples are reported where the SO_2NH functionality has to be alkylated before inducing the cyclization reaction.[4,9]

We present here the results of our investigations on the possibility to induce cyclization without the need of electron-withdrawing groups located on the para-position with respect

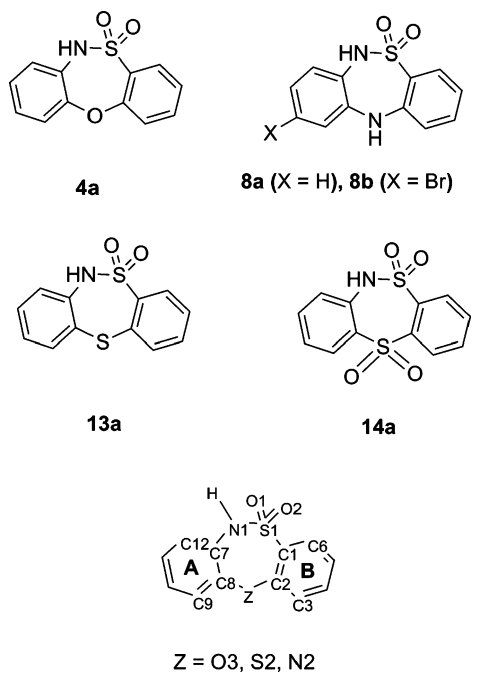

Fig. 3 Schematic drawings of the monomer molecules studied by single-crystal X-ray diffraction (**4a**, **8b**, **13a**, **14a**) and by computational methods (**4a**, **8a**, **13a**, **14a**). Inset drawing with the most relevant atom labelling.

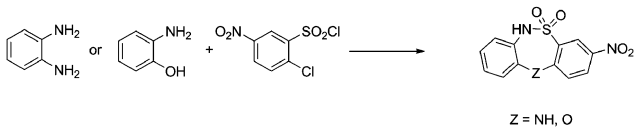

Scheme 1 Sulfonamide syntheses from previous literature.

to the leaving group, and without the need to alkylate the sulfonamide. The synthesis of these molecules is often complicated by the potential formation of the corresponding dimers; this side reaction can not be suppressed by dilution of the reaction mixture. For each of the nuclei discussed here a customized methodology is described.

Synthesis of dibenzoxathiazepine 5,5-dioxide. Only a few examples of dibenzoxathiazepine 5,5-dioxide compounds were synthesized in the past with different procedures.[6,10] Our general method to prepare these compounds is outlined in Scheme 2. Reaction of substituted 2-aminophenols **1a–j** with 2-bromobenzenesulfonyl chloride **2**, in pyridine, gave sulfonamides **3a–j**, that were cyclized in *N*-methylpyrrolidone (NMP) in the presence of cesium carbonate to the corresponding tricyclic sulfonamides **4a–j**. The structure of **4a** was confirmed by single-crystal X-ray analysis. Considering the drastic experimental conditions (140 °C and 20 h of reaction time) we evaluated the possible use of copper to promote the reaction, as in the Ullmann ether synthesis for the formation of diaryl ethers.[11] However, when elemental copper was added to the reaction mixture, only dimeric products were obtained. In particular, in the case of the cyclization of sulfonamide **3b**, the dimer **5b** was obtained, whose structure was confirmed by X-ray crystal structure analysis.

Synthesis of dibenzothiadiazepine 5,5-dioxides. The synthesis of unsubstituted dibenzothiadiazepine 5,5-dioxides was evaluated in various experimental conditions such as Ullmann-type copper-mediated procedures and Pd-catalyzed cross-coupling reactions. Some Pd-catalyzed cross-coupling experiments, made according to the described intramolecular palladium-catalyzed arylations,[12] are ineffective in the synthesis of these substances. Only the copper-catalyzed reactions gave rise to

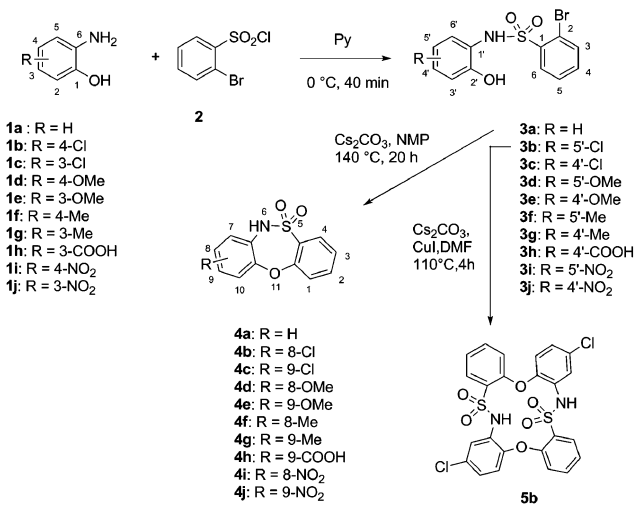

Scheme 2 Synthesis of dibenzoxathiazepine 5,5-dioxide.

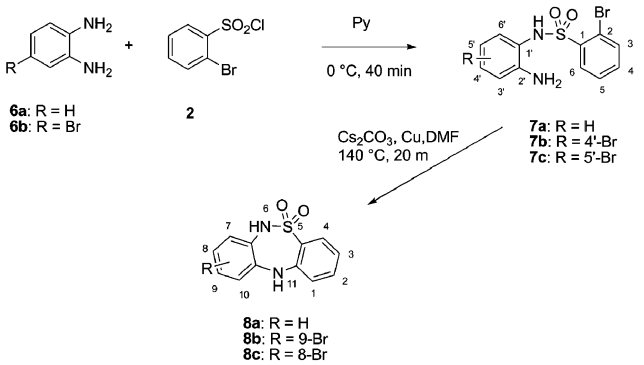

Scheme 3 Synthesis of dibenzothiadiazepine 5,5-dioxides.

the formation of the desired products and the preferred solvent was *N*,*N*-dimethylformamide (DMF).

The dibenzothiadiazepine 5,5-dioxides were obtained according to Scheme 3: the phenylenediamines **6a,b** were reacted with **2** in pyridine to form the sulfonamides **7a–c**: in the case of the bromo-substituted phenylenediamine **6b**, the two sulfonamides **7b** and **7c** were formed in the ratio 3 : 1. These products were cyclized in DMF in the presence of Cs_2CO_3 and Cu at 140 °C in a few minutes. The dibenzothiadiazepine 5,5-dioxides **8b** and **8c** were formed in the same ratio 3 : 1 as the open sulfonamides **7b** and **7c**; the structure of the main product **8b** was confirmed by X-ray analysis.

Synthesis of dibenzodithiazepine 5,5-dioxides. The dibenzodithiazepine 5,5-dioxides **13a,b** and their oxidized counterparts **14a,b** are new structures. Only an unsuccessful attempt to prepare the dibenzodithiazepine 5,5 dioxide was reported by thermolysis of diphenyl sulfide-2-sulfonyl azide.[10] We instead obtained **13a,b** by Ullmann-type reaction in good yields (Scheme 4). The sensitivity of sulfides towards oxidation holds some difficulties and the suppression of disulfide formation remains the main challenge for this type of reaction.[11] The desired cyclic compounds were obtained by using copper together with a reducing agent as Cu_2O, in order to inhibit the disulfide formation, and avoiding the use of strong bases as Cs_2CO_3. The use of a combination of copper and cuprous oxide in 2-ethoxyethanol suppressed the disulfide formation and the cyclization occurred in good yield, even in the absence of the base. The starting 2-aminothiophenols **9a,b** were protected as benzyl thioether derivatives **10a,b** according to described procedures;[13] the subsequent reaction with **2** gave sulfonamides **11a,b**. These thio-derivatives were deprotected by treatment with a 1 M solution of BBr_3 in CH_2Cl_2 and cyclized by treatment with copper and cuprous oxide in refluxing 2-ethoxyethanol giving the products **13a,b**, expeditiously and in good yields. Only a little amount (5%) of the dimeric by-product **15a** was formed, whose structure was confirmed by X-ray analysis. Finally the treatment of derivatives **13a,b** with *m*-chloroperbenzoic acid (*m*CPBA) in CH_2Cl_2 gave sulfones **14a,b** (Scheme 4). Structures of **13a** and **14a** were also confirmed by X-ray analysis.

Structural investigations

In the solid state (data retrieved from the Cambridge Structural Database,[14] CSD hereafter) unconstrained sulfonamides

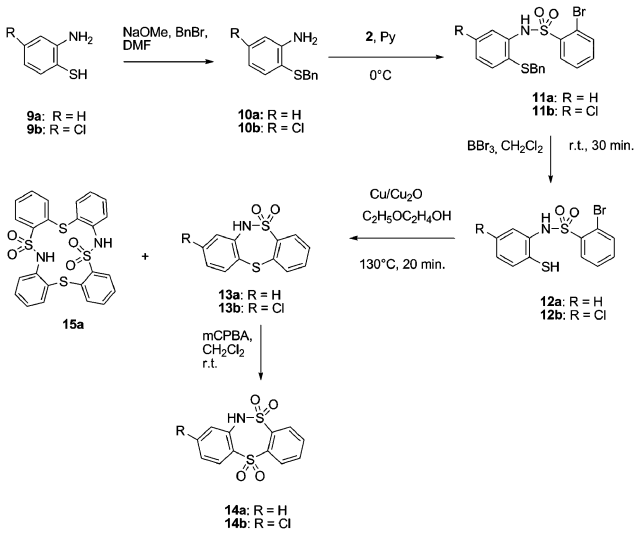

Scheme 4 Synthesis of dibenzodithiazepine 5,5-dioxides.

adopt a staggered conformation about the N–S bond (Scheme 5),[15] while the energy minimum gas-phase conformation predicted by high-level quantum mechanical studies has the NH and NC bonds almost eclipsing the SO linkages.[16] For example for *N*-methylmethanesulfonamide, the two conformers differ by 1.44 and 2.63 kcal mol^{-1} at the RHF/6-31G*[16b] and MP2/6-31 + G*[16d] level, respectively; while its crystal structure, collected at 150 K, shows the staggered conformation.[17] By the way, high-level *ab initio* calculations have been used to develop force field parameters for the sulfonamide derivatives.[16a,b,d]

It has been suggested that the gas-phase low energy conformation found in simple sulfonamides is mainly due to the resonance interaction between S=O bonds and the nitrogen electron lone pair:[18] the perpendicular orientation of the latter with respect to the S=O bond allows an optimal overlap between the nitrogen doublet and the S=O bonds. The reason why the minimum-energy conformation in the gas phase is not the minimum-energy conformation in the solid state as well, can be most likely ascribed to intermolecular hydrogen bonds and packing forces which, in the crystal, prevail over "intramolecular effects". Finally as a consequence of the uncertainty in the minimum-energy conformation, doubts can be cast on the choice of the solution conformation selected for modelling studies performed in solution. Because the results of the latter are crucial for drug design conclusions should be drawn with care.

When the sulfur and the nitrogen atoms bear a bulkier substituent, such as an aryl moiety, as for example in the

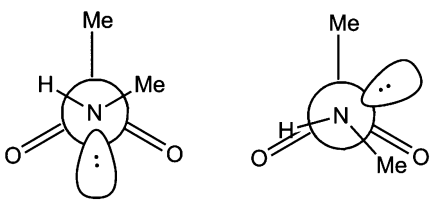

Scheme 5 Newman projections about the N–S bond for *N*-methylmethanesulfonamide: the experimentally solid-state observed structure (left) and the theoretical minimum energy conformation (right).

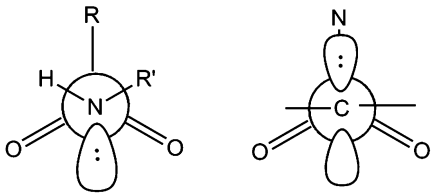

a b

Scheme 6 (a) Newman projections about the N–S bond of the solid-state lowest energy conformation for arylsulfonamide derivatives (R = Ar; R′ = alkyl) and *N*-arylmethanesulfonamide (R = methyl; R′ = Ar); (b) Newman projections about the C–S rotatable bond of the solid-state lowest energy conformation in arylsulfonamide derivatives (R = Ar; R′ = alkyl).

arylsulfonamides and *N*-arylmethanesulfonamides, respectively, the N lone pair still bisects the OŜO angle (Scheme 6(a)) in their solid-state conformation (CSD data and ref. 19). Moreover, in the arylsulfonamides the p orbital at the *ipso* carbon also bisects the OŜO angle (Scheme 6(b)). It has been hypothesized that the arylsulfonamides conformation is the result of the stabilizing interaction between the lone pairs and the sulfur d orbitals.[20] When a non-hydrogen atom (nH) is in *ortho* position, the peak of the N–S–C–C_{nH} dihedral distribution moves to about 70°.[19]

Results from quantum chemical calculations studies are in good agreement with these experimental findings. For example the most stable conformer of benzene sulfonamide has the S–N bond perpendicular to the benzene ring (the NH_2 group is eclipsing the SO_2 moiety);[21] while the presence of a methyl *ortho* substituent causes a rotation of 30° of the SO_2NH_2 grouping (the N–S–C–C_{nH} dihedral has a *gauche* conformation).[22]

Few crystal structures of cyclic six-, seven- and eight-membered sulfonamides have been retrieved from the CSD (Scheme 7 shows the molecular fragments searched for and the number of refcodes selected for the present study). In the smallest ring the "sulfa" group shows the usual 3D-arrangement about the N–S bond: the nitrogen lone pair bisects the OŜO angle: the absolute value of the dihedral angle τ_1 defined by the carbon atoms belonging to the ring is about 60°. The medium and the largest sized rings show conformations distributed in a broader range, with mean $|\tau_1|$ values higher.

We report here an experimental and theoretical structural analysis of compounds **4a**, **8b** (**8a**), **13a** and **14a** sketched in Fig. 3 with the aim to elucidating their conformational behaviour. The solid-state characterization by X-ray diffraction

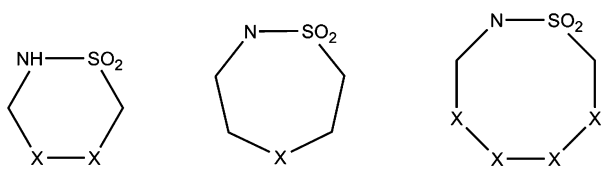

a b c

Scheme 7 Molecular fragments searched for in the CSD, v5.30 (2009): (a) 34 refcodes selected; (b) 8 refcodes selected; (c) 5 refcodes selected; X = any non-metal element; — any kind of bond.

was also extended to the dimer species **5b** (Scheme 2) and **15a** (Scheme 4).

Solid-state characterization results. The analysis and the discussion of the structural features characterizing the tricyclic compounds **4a**, **8b**, **13a** and **14a** (Fig. 4–7) have been focussed on the overall shape of the molecules rather than be limited to the geometry of the sulfonamide grouping.

Their overall structure is essentially controlled both by the conformation of the central seven-membered ring and the relative arrangement of the fused aromatic moieties about it.

The geometrical data as derived by X-ray measurements listed in the last column of Tables 1–4 help to quantify similarities and differences between the solid-state structures of samples **4a**, **8b**, **13a** and **14a**. As far as the 7-membered ring is concerned, the asymmetry index ΔC_s,[23,24] the bow and stern parameters[23,24] and the sum of the ring internal angles were taken into account. In addition, the bending of the two aromatic groups with respect to the central ring was measured by the angles their mean planes form with the plane passing through N1, S1 and Z (τ_3); whereas the relative arrangement of the phenyls was quantified by measuring the angle between their mean planes ($\angle$(A/B) value).[4c]

The geometry of the sulfonamide grouping was defined by all the C–NH–SO_2–C bond distances (see also ESI†), the sum of the angles about the N1 atom and finally by the dihedral angles τ_1 (C7–N1–S1–C1) and τ_2 (C6–C1–S1–N1).

A comparative inspection of the numerical data reported in Tables 3 and 4 highlights that compounds **13a** and **14a** (Fig. 6 and 7) are very similar both in their resulting overall shape (see for example τ_3, ΔC_s, bow and stern values) and in the sulfonamide arrangement (see for example τ_1, τ_2 and the degree of pyramidalization of N1 evaluated on the basis of the sum of the bond angles about it). In particular the conformation about the N–S bond (Scheme 8, left) is in keeping with the solid-state conformation observed in sulfonamides bearing aryl substituents (Scheme 6(a)), that is the nitrogen lone pair bisects the OŜO angle. On the contrary the dihedral about the C–S linkage is rotated about 90° (Scheme 8, right) with respect to the literature reference value (Scheme 6(b)). As a whole the solid-state geometry shown by **13a** and **14a** will be, hereafter, labelled as type **III**.

In both cases the hydrogen atom bound to N1 points towards the central seven-membered ring. In **14a** a weak

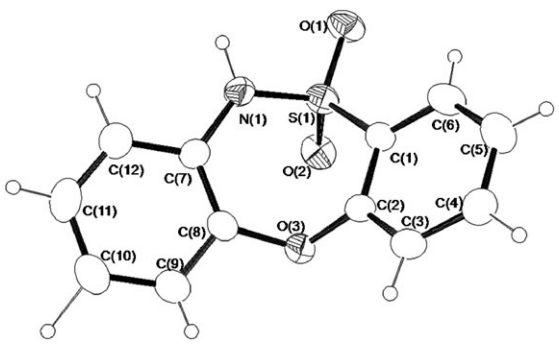

Fig. 4 ORTEP3 view of compound **4a**. The ellipsoid probability is set to 30%.

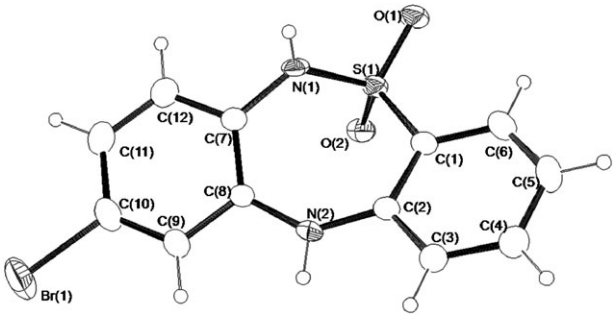

Fig. 5 ORTEP3 view of compound **8b**. The ellipsoid probability is set to 30%.

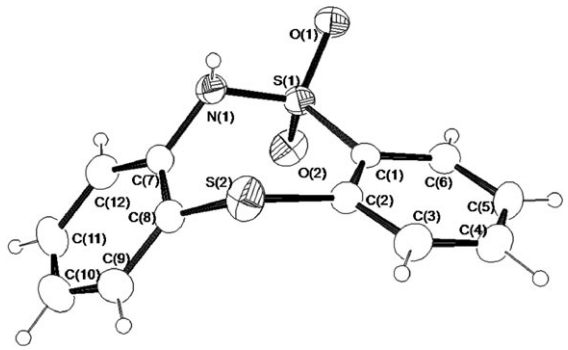

Fig. 6 ORTEP3 view of compound **13a**. The ellipsoid probability is set to 30%.

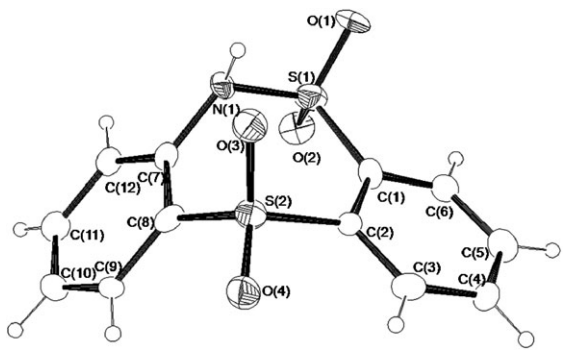

Fig. 7 ORTEP3 view of compound **14a**. The ellipsoid probability is set to 30%.

H-bond interaction (the NH···OSO distance is 2.53(8) Å, the angle 110(3)°) could contribute to further stabilize this 3D arrangement.

Fig. 6 and 7 highlight the overall shape of the molecules **13a** and **14a**, which appears quite folded about the central ring (∠(A/B) value), with the N1–S2 direction acting as a sort of hinge between the two molecular fragments which as a whole define a convex figure. Finally the seven-membered ring is quite asymmetric, as provided by the high value of the asymmetry indexes.

In both the oxo (**4a**) and amine (**8b**) derivatives, and at variance with the retrieved published data, the nitrogen atom N1 is almost planar trigonal (Scheme 8 left and Tables 1 and 2)

Table 1 Most relevant geometrical parameters (distances (Å), angles (°)) as derived from *ab initio* geometry optimizations (HF/6-311+G(d,p) level of theory) of the **4a-I**, **4a-II**, **4a-III** modelled species.[a] Those derived from X-ray diffraction data of **4a** have been also reported for comparative purposes

	4a-I	4a-II	4a-III	4a
r_{N1-S1}/Å	1.635	1.635	1.633	1.616(3)
r_{S1-O1}[b]/Å	1.423	1.423	1.422	1.426(2)
r_{S1-O2}/Å	1.415	1.415	1.419	1.434(2)
∑(∠N1)[c]/°	354.4	354.4	345.7	359(2)
τ_1[d]/°	−58.9	−59.0	−55.8	−62.1(3)
τ_2[e]/°	−121.5	−121.5	−178.8	−122.1(3)
τ_3[f]/°	12.5/59.9	12.6/59.9	55.7/2.3	16.3(1)/58.1(1)
∠(A/B)[g]/°	48.9	48.9	54.5	45.5(1)
ΔC_s[h]/°	42.0	42.0	46.3	50.0
Bow[h]/°	54.5	54.5	55.2	50.6(3)
Stern[h]/°	30.7	30.7	25.1	40.4(1)

[a] Refer to Fig. 3 for molecular models and atom labelling. [b] O1 is the sulfone oxygen atom closest to the N-bound hydrogen. [c] Summation of the bond angles about the sulfonamide nitrogen atom N1. [d] C7–N1–S1–C1 Dihedral angle. [e] C6–C1–S1–N1 Dihedral angle. [f] Angles between the plane through N1, S1, Y and the least-squares planes through rings A and B, respectively. [g] Interplanar angle between the aromatic rings. [h] See ref. 23 and 24 for the parameter definitions.

Table 2 Most relevant geometrical parameters (distances (Å), angles (°)) as derived from *ab initio* geometry optimizations (HF/6-311+G(d,p) level of theory) of the **8a-I**, **8a-II**, **8a-III** modelled species.[a] Those derived from X-ray diffraction data of **8b** have been also reported for comparative purposes

	8a-I	8a-II	8a-III	8b
r_{N1-S1}/Å	1.630	1.643	1.630	1.596(4)
r_{S1-O1}[b]/Å	1.423	1.424	1.423	1.435(3)
r_{S1-O2}/Å	1.420	1.423	1.420	1.426(3)
∑(∠N1)[c]/°	347.0	347.0	346.6	359(3)
τ_1[d]/°	−65.0	−84.0	−64.8	−81.3(3)
τ_2[e]/°	−168.1	−145.5	−168.3	−132.0(3)
τ_3[f]/°	55.3/13.8	54.3/38.6	55.3/13.6	39.0(1)/49.1(2)
∠(A/B)[g]/°	44.1	28.6	44.3	21.5(1)
ΔC_s[h]/°	53.6	68.0	53.4	65.7
Bow[h]/°	45.9	23.5	46.1	9.7(4)
Stern[h]/°	19.6	9.1	19.8	28.7(2)

[a] Refer to Fig. 3 for molecular models and atom labelling. [b] O1 is the sulfone oxygen atom closest to the N-bound hydrogen. [c] Summation of the bond angles about the sulfonamide nitrogen atom N1. [d] C7–N1–S1–C1 Dihedral angle. [e] C6–C1–S1–N1 Dihedral angle. [f] Angles between the plane through N1, S1, Y and the least-squares planes through rings A and B, respectively. [g] Interplanar angle between the aromatic rings. [h] See ref. 23 and 24 for the parameter definitions.

and the NH bond, which eclipses a SO linkage, is directed outside the molecular skeleton. The p orbital of the S-bound aromatic carbon results nearly perpendicular to a S=O bond in keeping with the literature concerning bulky solfonamides. (Scheme 8 right and Tables 1–2). Besides, compounds **4a** and **8b** differ in their overall shape: the amine derivative (**8b**, Fig. 5) is almost flat (see for example the ∠(A/B) angular value), and

Table 3 Most relevant geometrical parameters (distances (Å), angles (°)) as derived from *ab initio* geometry optimizations (HF/6-311+G(d,p) level of theory) of the **13a-I**, **13a-II**, **13a-III** modelled species.[a] Those derived from X-ray diffraction data of **13a** have been also reported for comparative purposes

	13a-I	13a-II	13a-III	13a
r_{N1-S1}/Å	1.634	1.634	1.632	1.610(3)
r_{S1-O1}[b]/Å	1.424	1.424	1.422	1.432(2)
r_{S1-O2}/Å	1.415	1.415	1.420	1.428(2)
$\sum(\angle N1)$[c]/°	359.3	359.4	346.0	346(2)
τ_1[d]/°	−74.6	−74.1	−53.6	−69.4(2)
τ_2[e]/°	−117.0	−116.9	167.7	−173.0(2)
τ_3[f]/°	18.4/65.0	17.9/65.0	56.9/11.7	58.7(1)/7.4(1)
$\angle$(A/B)[g]/°	47.9	48.3	68.2	51.6(1)
ΔC_s[h]/°	59.3	59.0	43.7	50.6
Bow[h]/°	42.5	42.7	49.2	43.2(1)
Stern[h]/°	31.9	32.1	33.5	12.1(1)

[a] Refer to Fig. 3 for molecular models and atom labelling. [b] O1 is the sulfone oxygen atom closest to the N-bound hydrogen. [c] Summation of the bond angles about the sulfonamide nitrogen atom N1. [d] C7–N1–S1–C1 Dihedral angle. [e] C6–C1–S1–N1 Dihedral angle. [f] Angles between the plane through N1, S1, Y and the least-squares planes through rings A and B, respectively. [g] Interplanar angle between the aromatic rings. [h] See ref. 23 and 24 for the parameter definitions.

Table 4 Most relevant geometrical parameters (distances (Å), angles (°)) as derived from *ab initio* geometry optimizations (HF/6-311+G(d,p) level of theory) of the **14a-I**, **14a-II**, **14a-III** modelled species.[a] Those derived from X-ray diffraction data of **14a** have been also reported for comparative purposes

	14a-I	14a-II	14a-III	14a
r_{N1-S1}/Å	1.638	1.638	1.627	1.594(7)
r_{S1-O1}[b]/Å	1.421	1.420	1.417	1.424(4)
r_{S1-O2}/Å	1.412	1.412	1.419	1.446(6)
$\sum(\angle N1)$[c]/°	355.2	355.2	347.5	348(2)
τ_1[d]/°	−86.6	−86.7	−60.7	−62.9(6)
τ_2[e]/°	−120.4	−120.5	174.8	178.0(5)
τ_3[f]/°	31.5/65.5	31.6/65.5	25.8/38.4	59.1(3)/2.9(2)
$\angle$(A/B)[g]/°	39.9	39.8	64.1	60.5(2)
ΔC_s[h]/°	45.6	45.6	50.3	53.4
Bow[h]/°	32.3	32.2	48.8	45.8(3)
Stern[h]/°	27.4	27.4	28.4	20.4(4)

[a] Refer to Fig. 3 for molecular models and atom labelling. [b] O1 is the sulfone oxygen atom closest to the N-bound hydrogen. [c] Summation of the bond angles about the sulfonamide nitrogen atom N1. [d] C7–N1–S1–C1 Dihedral angle; [e] C6–C1–S1–N1 Dihedral angle. [f] Angles between the plane through N1, S1, Y and the least-squares planes through rings A and B, respectively. [g] Interplanar angle between the aromatic rings. [h] See ref. 23 and 24 for the parameter definitions.

its shape results definitely more "open" with respect to **13a** and **14a**; while compound **4a** (Fig. 4) shows a concave shape (*vs.* the convex one featuring **13a** and **14a**), folded about the N1–O3 direction. As a whole the solid-state arrangements of **4a** and **8b** will be labelled as type **I** and type **II**, respectively. Molecule **8b** shows by far the most asymmetric central ring (ΔC_s = 65.7 *vs.* 50.0° (for **4a**), 50.6° (for **13a**) and 53.4° (for **14a**).

Concerning the crystal packing, all the four tricyclic compounds **4a**, **8b**, **13a** and **14a** are held together in the lattice by a net of hydrogen bonds (see ESI†).

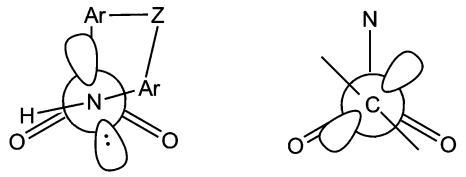

4a (Z = O, type **I** geometry), **8b** (Z = NH, type **II** geometry)

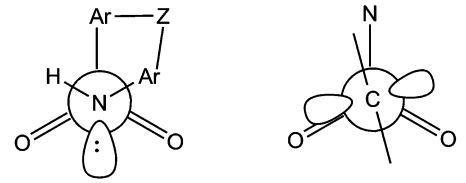

13a (Z=S), **14a** (Z=SO_2) (type **III** geometry)

Scheme 8 Newman projections about the N–S and C–S bonds showing the different conformations in the X-ray solid-state structures of molecules **4a**, **8b**, **13a**, **14a**.

Dimeric compounds **5b** and **15a** are in a "sandwich-like" conformation (see Fig. 8 and 9) characterized by π–π interactions[25] involving the aromatic rings A and A′ (see Fig. 8 and 9). The latter are almost parallel each others (the angle between their mean planes is 6.5(2) and 10.7(3)° for **5b** and **15a**, respectively) with their centroids at 3.914(4) and 3.66(1) Å in **5b** and **15a**, respectively, and almost perpendicular with respect to the other two aromatic rings B and B′. The mean planes defined by the carbon atoms of the latter form an angle of 46.1(2) and 30.1(3)° in **5b** and **15a**, respectively. The "sulfa" grouping shows the expected conformation about both the S–N and C–S bonds.

In both the crystal lattices the oxygen atom O(1s) of the crystallization Me_2SO (DMSO) molecule acts as a bidentate acceptor of H-bonds with respect to the hydrogen atoms bound to N(1a) and N(1b) (see ESI†).

In summary the solid-state conformation about the N–S bond found in the oxo (**4a**) and amine (**8b**) derivatives is rather unusual with respect both to the literature data and that

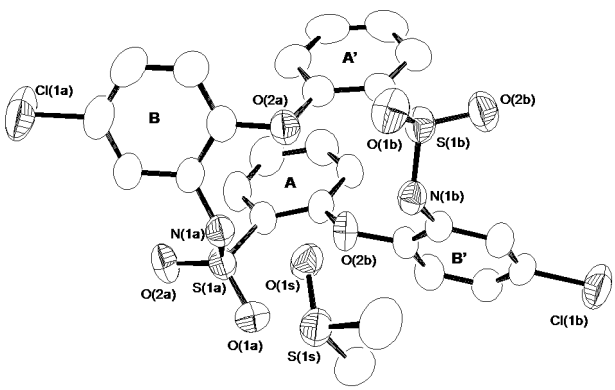

Fig. 8 ORTEP3 view of **5b**·Me_2SO. The ellipsoid probability is set to 30%.

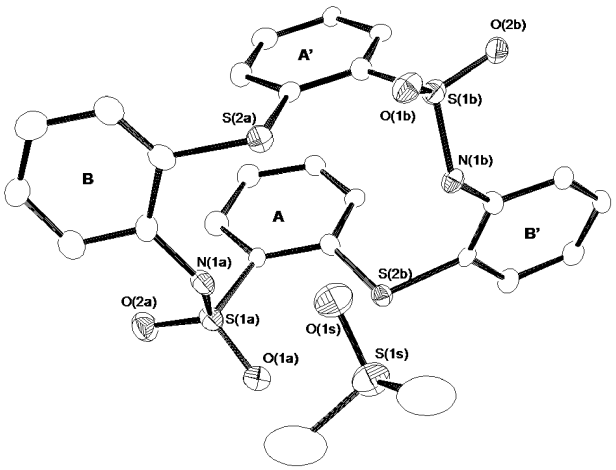

Fig. 9 ORTEP3 view of compound **15a**·Me_2SO. The ellipsoid probability is set to 30%.

shown by the sulfur compounds (**13a** and **14a**). The reverse holds for the arrangement about the C–S bond which for the lightest **4a** and **8b** species is in keeping with the reported data, while in the sulfur derivatives the S-bound aromatic ring almost eclipses the N–S bond.

Computational study results. With this in mind we set up a modelling study aiming to finding a rationale for the solid-state data and eventually to investigate if there exists any correlation between the observed geometry and the nature of the Z grouping (O, NH, S, SO_2). For each molecule (**4a**, **8a**, **13a** and **14a**, Fig. 3) three different starting geometries (**I**, **II** and **III**) were taken into account for the subsequent fully optimization by the quantum chemical procedures (details in the experimental section). Tables 1–4 list the most interesting geometrical parameters related to the optimized structures (**4a-I**/**4a-III**, **8a-I**/**8a-III**, **13a-I**/**13a-III**, **14a-I**/**14a-III**). Results are summarized in the following.

As a general remark, in all the optimized species the N–S bond distances are larger than the experimental values. The same trend is almost invariably observed for the S–O1 bond with respect to the S–O2 one (see Tables 1–4). The most stable conformation is always of type **III** (see Table 5) where the sulfonamide nitrogen features an sp^3 hybridization (mean $\sum(\angle N1) = 346°$) with the nitrogen lone pair bisecting the SO_2 angle (as in the bulky unconstrained species, Scheme 6) and the S-bound phenyl ring parallel with respect to the S–N bond. As a final remark, the type **III** conformer is increasingly stabilized on going from NH → O → S → SO_2 (0.67, 1.29, 3.3, 9.4 kcal mol^{-1}, respectively, Table 5).

Table 5 HF/6-311+G(d,p)//HF/6-311G+(d,p) energy difference (kcal mol^{-1}) with respect to the most stable conformer for each modelled compound

	I	II	III
4a	+1.29	+1.29	0.0
8a	0.0	+0.67	0.0
13a	+3.3	+3.3	0.0
14a	+9.4	+9.4	0.0

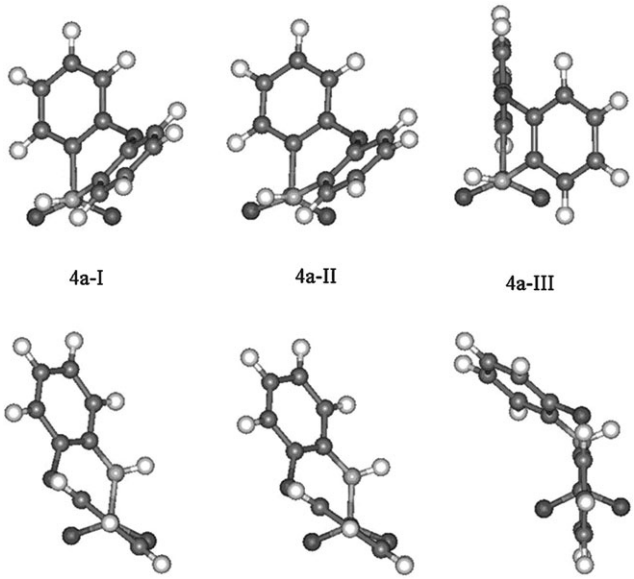

Fig. 10 Newman projections about the N–S (top) and C–S (bottom) bonds of the optimized **4a-I**/**4a-III** models.

For compounds **4a**, **13a** and **14a** the minimization procedure makes geometry of type **II** transform into **I** as provided by a comparison of the geometrical parameters featuring the optimized models **4a-I** and **4a-II** (Table 1, Fig. 10), **13a-I** and **13a-II** (Table 3, Fig. 12), **14a-I** and **14a-II** (Table 4, Fig. 13). In all cases the optimized conformer **I** is characterized by an almost planar sulfonamide nitrogen (mean $\sum(\angle N1) = 356°$) with the bound hydrogen practically eclipsing one SO bond and closely resembles the experimental solid-state structure of **4a**; while the optimized conformer **III** (the most stable) well reproduces the experimental structure of the sulfur (**13a**) and sulfone (**14a**) derivatives.

As to the **8a** species, the geometry optimization of **8a-I** proceeds through the inversion of both the nitrogen atoms and

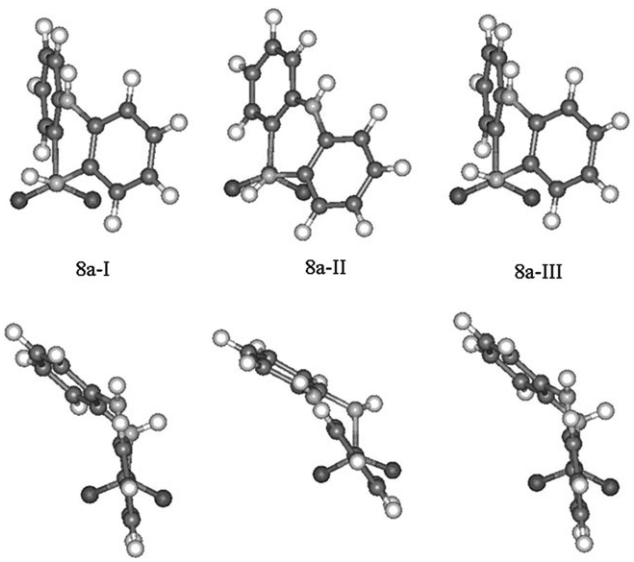

Fig. 11 Newman projections about the N–S (top) and C–S (bottom) bonds of the optimized **8a-I**/**8a-III** models.

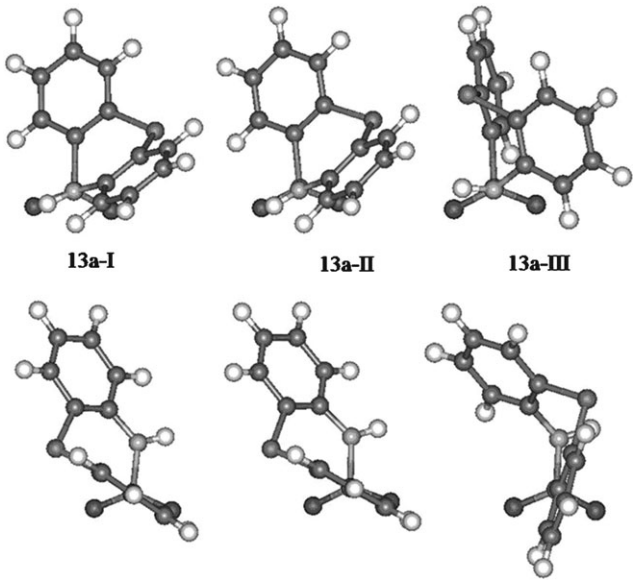

Fig. 12 Newman projections about the N–S (top) and C–S (bottom) bonds of the optimized **13a-I**/**13a-III** models.

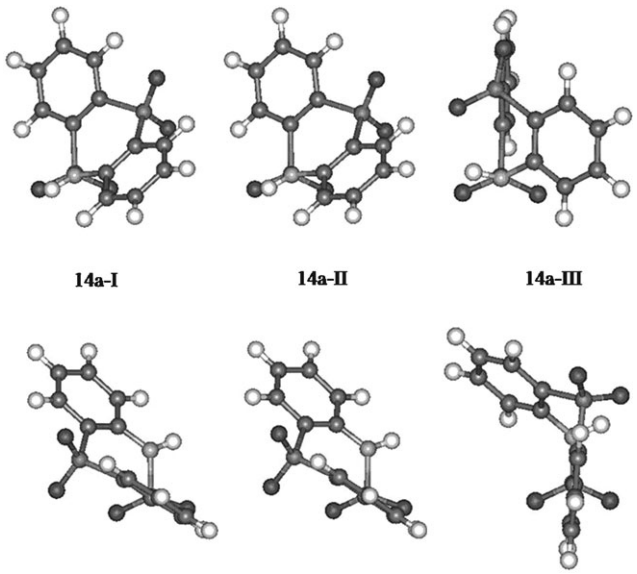

Fig. 13 Newman projections about the N–S (top) and C–S (bottom) bonds of the optimized **14a-I**/**14a-III** models.

results into the isoenergetic **8a-III** conformer (Table 2, Fig. 11). The optimized **8a-II** isomer looks like the experimental structure **8b**, except for the N1 hybridization (sp^3 in the former *vs.* sp^2 in the experimental structure) and it is 0.67 kcal mol^{-1} higher in energy than conformer **III**.

The convergence trends outlined above may suggest that type **II** geometry is somehow peculiar of the amine derivative **8a**, given that the geometry optimization of the #-**II** (# = **4a**, **13a** and **14a**) species leads in all cases to conformer **I**. As a consequence we can suppose that for the oxo, sulfur and sulfone derivatives there is a quite low energy barrier for the **II** → **I** transformation. Conformer **III** corresponds in all cases to the most thermodynamically stable and, most likely it is placed in a quite deep potential well.

In summary, while the solid-state geometry of the heavier derivatives **13a** and **14a** is well reproduced by the gas phase minimum-energy conformer **III**, the 3D arrangement shown by the oxo and amine derivatives in the solid state (**I** and **II**, respectively) appears slightly disfavoured on an energetic ground with respect to the lowest energy gas-phase conformer **III**.

The latter in all cases features an sp^3 hybridized amide nitrogen, while the experimental solid-state structures of **4a** and **8b** have a trigonal planar nitrogen. The Weinhold's Natural Bond Orbital (NBO)[26] analysis highlights that in all the optimized structures the nitrogen lone pair is partially delocalized over the neighbouring atomic groupings. In all cases, while the lone pair of the pyramidal nitrogen (type **III** conformer) is mainly delocalized on the S1–C1 σ* bond, when the nitrogen has sp^2 character, the p doublet moves in opposite direction being largely transferred to the π* orbital localized between C7–C8. The 3D arrangement about the S1–C1 bond in type **III** conformer and in the solid-state structures of **13a** and **14a** can be explained as the natural consequence of the lone pair delocalization and seven-membered ring closure. When the conjugation interests the N-bound phenyl (3D arrangement of **4a** and **4I-a**) the dihedral about the S1–C1 linkage has the usual value as expected in case of bulky substituents on the aryl fragment. As a final remark the transfer of the lone pair electron density appears more efficient when the doublet is hosted in an almost pure p orbital than in a sp^3 hybrid as implicitly suggested by the slightly larger electronic occupancy of the latter orbital. The stabilizing effect related to a more efficient electron density delocalization operating in conformer **I** could be important in determining the "sulfa" group conformation of the lightest derivative **4a** (its solid-state structure features an sp^2 nitrogen and conformer **4a-I** is only 1.29 kcal mol^{-1} higher in energy than **4a-III**). In the sulfur species **13a** and **14a**, which undoubtedly prefer conformer **III** (that is by far the gas phase most stable and it is the solid-state conformer) other factors must contribute to drive their 3D arrangement, as for example the SO_2–Z steric hindrance. In **14a** the oxygen atoms of the two sulfone groupings are 2.985 Å apart in conformer **I** *vs.* 3.972 Å in **III** (the sum of the oxygen van der Waals radii is 3.04 Å[27]). For comparison **13a-I** features an S···O distance of 3.173 *vs.* 4.210 Å in **13a-III** (the sum of the corresponding van der Waals radii is 3.32 Å). Results from geometry optimizations of two further molecular models having Z = CH_2 and $C(CH_3)_2$ could substantiate this hypothesis.[28] The first model (Z = CH_2) prefers the type **I** geometry (Δ(**I–III**) = −1.52 kcal mol^{-1}), while for the dimethyl derivative the reverse holds (Δ(**I–III**) = +2.99 kcal mol^{-1}).

Conclusions

In conclusion, through customized synthetic procedures we have obtained highly functionalizable sulfonamide tricyclic structures featuring NH, O, S and SO_2 groups in the central seven-membered ring, for which general and reproducible methods of synthesis were lacking. Furthermore, as sulfonamide-related conformational effects have been proposed to play a role in structure based drug design[8] and tricyclics are well know privileged structures in medicinal chemistry, attention

has been paid to the 3D arrangement of these molecules. Single-crystal X-ray diffraction data and quantum chemical studies allowed to compare the minimum energy geometries in the solid state (**I**, Z = O; **II**, Z = NH and **III**, Z = S, SO_2) with the minimum-energy geometries in the gas phase (invariably the type **III** geometry). The results, which are interpreted on the basis of both the efficiency in the amide nitrogen lone pair delocalization and of the SO_2–Z steric hindrance, possibly lead to a better understanding of the three-dimensional arrangement of these molecules that could be helpful in the study of their interactions with their biological targets.

Experimental

Synthesis

All reagents and solvents were used without further purification or drying and were purchased from Sigma-Aldrich (Milan, Italy). Melting points were measured in capillary tubes with a digital electrothermal apparatus Buchi B-540 and were uncorrected. TLC monitoring was performed on Merck silica gel 60 F_{254} plates and detection by UV light. HPLC chromatograms were recorded on a Agilent HP-1100 instrument using the following method: Zorbax™ columm SB-18, 3.5 mμ, 100 Å (50 × 4.6 mm). Mobile phase: A, trifluoroacetic acid 0.1% in water; B, trifluoroacetic acid 0.1% in acetonitrile; gradient from 5% B to 95% B in 6.5 min, then 95% B for 1 min; flow: 3 mL min^{-1}; wavelength 1: 210 nm, wavelength 2: 270 nm.

^{1}H NMR spectra were acquired at 600 MHz on a Bruker AC 600 spectrometer or on a Varian Gemini 200 spectrometer and referenced against the residual solvent peak (DMSO-d_6 at 2.50 ppm and $CDCl_3$ at 7.25 ppm). All processing were performed using the software *Mestrec 4.5.9.1*. Mass spectra were obtained with a Finnigan LCQ ion trap mass spectrometer, operated in positive-ion or in negative-ion electrospray ionization. The samples were analyzed by full-scan MS and product ion MS/MS of the quasi-molecular ions, at 30% relative collision energy, using helium as the collision gas. The high-resolution mass spectra were obtained with a Micromass Q-Tof micro mass spectrometer, calibrated with 0.1% phosphoric acid in 1 : 1 H_2O–MeCN. This same mixture was used also as internal reference compound during ESI-MS accurate mass experiments, and was introduced *via* the Lock-Spray channel using an infusion pump. Ionization mode: ESI, positive or negative ion. Scan mode: full-scan MS from m/z 100 to 1000; capillary voltage: 3300 V; capillary temperature: 150 °C; source temperature: 80 °C; cone gas: nitrogen, 50 L h^{-1}. Sample introduction: direct infusion through the built-in syringe pump, flow 5 mL min^{-1}.

EI mass spectra were obtained with an Agilent 5973 GC-MS system, using an HP-5-MS open tubular capillary column, 15 m length, 0.25 mm internal diameter, 0.1 μm film thickness. The oven temperature was set at 60 °C for 3 min, then ramped at 50 °C min^{-1} up to 310 °C, and held at the final temperature for 2 min. 1 μL of the sample solution was injected in split mode, with a split ratio 1 : 100. The carrier gas was helium at 1.0 mL min^{-1}. The injector temperature was 250 °C.

2-Bromo-*N*-(2-hydroxyphenyl)benzenesulfonamide 3a. To a stirred solution of 2-aminophenol **1a** (2.20 g, 20 mmol) in dry pyridine (40 mL) at 0 °C, under an atmosphere of dry nitrogen, 2-bromobenzenesulfonyl chloride **2** (5.11 g, 20 mmol) was added portionwise. The reaction mixture was stirred for 0.5 h at 0 °C and 1 h at room temperature, then the solvent was removed under reduced pressure. The residue was diluted with an aqueous 1 M HCl solution and extracted with CH_2Cl_2. The organic phase was washed with brine, dried on phase separator. After removal of the solvent **3a** (5.93 g, 90%) was obtained as a solid.

HPLC: 3.65 min. ^{1}H NMR (200 MHz, DMSO-d_6): δ 9.45 (br s, 1H), 8.00–7.89 (m, 1H), 7.88–7.77 (m, 1H), 7.55–7.44 (m, 2H), 7.11–7.02 (m, 1H), 6.98–6.86 (m, 1H), 6.80–6.60 (m, 2H). ESI$^-$ $[M - H]^-$ = m/z 326.

Compounds **3b–j** were obtained with a similar procedure.

6*H*-Dibenzo[*b*,*f*][1,4,5]oxathiazepine 5,5-dioxide 4a. A solution of compound **3a** (1.22 g, 3.71 mmol) in 1-methyl-2-pyrrolidone (40 mL) was treated with cesium carbonate (3.63 g, 11.14 mmol). The mixture was heated at 140 °C for 20 h, then the solvent was removed under reduced pressure. The residue was diluted with an aqueous 1 M HCl solution and extracted with CH_2Cl_2. The organic phase was washed with brine, dried on phase separator. After removal of the solvent a crude oil was obtained, which was purified by flash chromatography (cyclohexane–ethyl acetate 2 : 1) using column STRATA SiO_2 (50 g) to give **4a** (590 mg, 64.3%) as a solid, mp 132–133 °C (from ethyl ether–hexane). TLC: R_f (ethyl acetate–cyclohexane: 1 : 2) = 0.46. HPLC: 3.42 min, 98.0% purity. ^{1}H NMR (600 MHz, DMSO-d_6): δ 10.85 (s, 1H), 7.80–7.76 (m, 1H), 7.74–7.69 (m, 1H), 7.52–7.48 (m, 1H), 7.44–7.40 (m, 1H), 7.38–7.44 (m, 1H), 7.20–7.14 (m, 2H), 7.08–7.04 (m, 1H). ESI$^-$ $[M - H]^-$ = m/z 246. HRMS: m/z 246.0226 ($[C_{12}H_9NO_3S–H]^-$; calc. 246.0227).

Compounds **4b–j** were obtained with a similar procedure.

2,13-Dichloro-11*H*,22*H*-5,16-dioxa-10,21-dithia-11,22-diazatetrabenzo[*a*,*d*,*h*,*k*]cyclotetradecene 10,10,21,21-tetraoxide 5b. A solution of compound **3b** (0.72 g, 2 mmol) in DMF (40 mL) was treated with cesium carbonate (1.90 g, 6 mmol) and CuI (20 mg, 0.1 mmol). The mixture was heated at 110 °C for 4 h. After cooling, the reaction mixture was diluted with an aqueous 1 M NaOH solution and the insoluble substance filtered off. The filtrated solution was acidified with 1 M HCl and an insoluble material was recovered by filtration. A crude solid was obtained, which was purified by flash chromatography (SiO_2) and eluted using 20% of ethyl acetate in hexane to give **5b** as a solid (0.07 g, 6%). HPLC: 4.96 min. ^{1}H NMR (600 MHz, $CDCl_3$): δ 9.72 (br s, 2H), 7.78 (d, J = 2.5 Hz, 2H), 7.76–7.72 (m, 2H), 7.2 (dd, J = 2.5, 8.7 Hz, 2H), 6.94 (d, J = 8.7 Hz, 2H), 6.91–6.85 (m, 4H), 5.76 (bd, J = 5.8 Hz, 2H). ESI$^-$ $[M - H]^-$ = m/z 561.

***N*-(2-Aminophenyl)-2-bromobenzenesulfonamide 7a.** To a stirred solution of benzene-1,2-diamine **6a** (2.70 g, 25 mmol) in dry pyridine (30 mL) at 0 °C, under an atmosphere of dry nitrogen, 2-bromobenzenesulfonyl chloride **2** (6.38 g, 0.025 mol) was added portionwise. The reaction mixture was stirred for 0.5 h at 0 °C and 1 h at room temperature, then the solvent was

removed under reduced pressure. The residue was diluted with an aqueous 1 M HCl solution and extracted with CH_2Cl_2 (900 mL) and again with CH_2Cl_2 (450 mL). The organic phase was washed with brine, dried on phase separator. After removal of the solvent the crude residue was washed with CH_2Cl_2 and **7a** (3.80 g, 46.5%) was obtained as a pure solid. HPLC: 2.82 min. ^{1}H NMR (200 MHz, DMSO-d_6): δ 7.93–7.79 (m, 2H), 7.57–7.40 (m, 2H), 6.94–6.79 (m, 1H), 6.71–6.56 (m, 2H), 6.41–6.26 (m, 1H). ESI$^+$ $[M + H]^+ = m/z$ 327. HRMS: m/z 326.9803 ($[C_{12}H_{11}N_2O_2SBr + H]^+$; calc. 326.9803).

***N*-(2-Amino-4-bromophenyl)-2-bromobenzenesulfonamide 7b and *N*-(2-amino-5-bromophenyl)-2-bromobenzenesulfonamide 7c.** Compounds **7b** and **7c** were obtained following the procedure described above for **7a** starting from **6b** (1.45 g, 7.75 mmol) and 2-bromobenzenesulfonyl chloride **2** (2.00 g, 7.84 mmol), in pyridine (15 mL) as a 3 : 1 mixture of regioisomers, which were separated by crystallization from MeOH in which **7b** is more soluble. After evaporation of the solvent, **7b** (1.50 g, 60%) was obtained. HPLC: 4.04 min. ^{1}H NMR (200 MHz, DMSO): δ 9.62 (br s, 1 H), 7.89–7.85 (m, 2 H), 7.59–7.47 (m, 2 H), 6.82–6.80 (m, 1 H), 6.61–6.48 (m, 2 H), 5.31 (br s, 2 H).

The product **7c**, insoluble in MeOH, was filtered off and isolated (0.50 g, 20%). HPLC: 3.89 min. ^{1}H NMR (200 MHz, DMSO-d_6): δ 7.92–7.85 (m, 2 H), 7.59–7.52 (m, 2 H), 7.06–7.00 (m, 1 H), 6.82–6.79 (m, 1 H), 6.59 (d, J = 8.7 Hz, 1 H), 5.33 (br s, 2 H).

6,11-Dihydrodibenzo[*c*,*f*][1,2,5]thiadiazepine 5,5-dioxide 8a. A solution of compound **7a** (0.90 g, 2.76 mmol) in *N*,*N*-dimethylformamide (40 mL) was heated at 140 °C and treated first with elemental copper (178 mg, 2.8 mmol) and then with cesium carbonate (0.90 g, 2.8 mmol). After 20 min at 140 °C, the reaction mixture was cooled with a cold water bath and, after filtration by suction, the filtered solution was evaporated to give a residue, that was dissolved in 1 M sodium hydroxide and washed with CH_2Cl_2. The aqueous solution was acidified with HCl and extracted with CH_2Cl_2. The organic phase was washed with brine, dried on a phase separator; after removal of the solvent a crude solid was obtained, which was purified by flash chromatography (CH_2Cl_2) using column STRATA SiO_2 (50 g) to give **8a** as a solid (430 mg, 63%), mp 198–199 °C. TLC: R_f (CH_2Cl_2–MeOH: 95/5) = 0.60. HPLC: 3.09 min, 99.7% purity. ^{1}H NMR (600 MHz, DMSO-d_6): δ 9.82 (s, 1H), 9.00 (s, 1H), 7.63–7.59 (m, 1H), 7.40–7.35 (m, 1H), 7.20–7.12 (m, 2H), 7.10–7.00 (m, 2H), 6.90–6.80 (m, 2H). ESI$^+$ $[M + H]^+ = m/z$ 247. HRMS: m/z 247.0541 ($[C_{12}H_{10}N_2O_2S + H]^+$; calc. 247.0541).

9-Bromo-6,11-dihydrodibenzo[*c*,*f*][1,2,5]thiadiazepine 5,5-dioxide 8b. Compound **8b** was prepared following the procedure described above for **8a** starting from **7b** (1.50 g, 3.70 mmol), Cu (0.60 g, 9.44 mmol) and Cs_2CO_3 (3.00 g, 9.23 mmol). The product **8b** (0.90 g, 75%) was obtained as a solid. HPLC: 3.68 min. ^{1}H NMR (200 MHz, DMSO-d_6): δ 9.99 (s, 1 H), 9.17 (s, 1 H), 7.62 (d, J = 7.9 Hz, 1 H), 7.46–7.38 (m, 1 H), 7.29–7.28 (m, 1 H), 7.17 (d, J = 8.2 Hz, 1 H), 7.04–6.84 (m, 3 H). ESI$^+$ $[M + H]^+ = m/z$ 325.

***N*-(2-Benzylsulfanylphenyl)-2-bromobenzenesulfonamide 11a.** To a stirred solution of **10a** (2.54 g, 11.79 mmol) in pyridine (25 mL), at 0 °C under an atmosphere of dry nitrogen, **2** (6.2 g, 25 mmol) was added portionwise. The reaction mixture was stirred at 0 °C for 2 h and for 16 h at room temperature, then the solvent was removed under reduced pressure. The residue was diluted with an aqueous 1 M HCl solution and extracted with CH_2Cl_2. The organic phase was washed with brine, an aqueous 5% $NaHCO_3$ solution, brine and then dried on phase separator and concentrated *in vacuo* to give **11a** (4.60 g, 90%) as a solid. TLC: R_f (ethyl acetate–hexane, 1 : 4) = 0.44. HPLC: 5.31 min. ^{1}H NMR (200 MHz, DMSO-d_6): δ 9.62 (s, 1H), 7.96–7.80 (m, 2H), 7.60–7.46 (m, 2H), 7.38–6.90 (m, 9H), 4.07 (s, 2H). ESI$^+$ $[M + H]^+ = m/z$ 434. HRMS: m/z 433.9879 ($[C_{19}H_{16}NO_2S_2Br + H]^+$; calc. 433.9884).

***N*-(2-Benzylsulfanyl-5-chlorophenyl)-2-bromobenzenesulfonamide 11b.** In a similar way, starting from **10b** (1.07 g, 4.3 mmol), **11b** was obtained (1.14 g, 56%) as a solid. HPLC: 5.68 min. ^{1}H NMR (200 MHz, DMSO-d_6): δ 9.90 (s, 1H), 7.98–7.82 (m, 2H), 7.64–7.50 (m, 2H), 7.39–6.98 (m, 8H), 4.07 (s, 2H). EI$^+$ $M^+ = m/z$ 467.

2-Bromo-*N*-(2-mercaptophenyl)benzenesulfonamide 12a. To a stirred solution of compound **11a** (4.30 g, 9.9 mmol) in dry CH_2Cl_2 (170 mL) at 0 °C, under an atmosphere of dry nitrogen, 1 M boron tribromide in CH_2Cl_2 was added, then the cold bath was removed and the reaction mixture was stirred for 30 min at room temperature. Brine was added to the reaction mixture and the crude product was extracted with CH_2Cl_2. The organic phase was treated with an aqueous solution of 1 M NaOH and the product was solubilized in the aqueous phase. Its subsequent acidification with concentrated HCl and extraction with CH_2Cl_2 gave, after washing with brine, drying on phase separator and evaporation *in vacuo*, **12a** as an oil (3.40 g, 100%).

HPLC: 4.18 min. ^{1}H NMR (200 MHz, $CDCl_3$): δ 8.20–8.12 (m, 1H), 7.97 (s, 1H), 7.75–7.76 (m, 1H), 7.50–6.90 (m, 6H), 3.24 (s, 1H).

2-Bromo-*N*-(5-chloro-2-mercaptophenyl)benzenesulfonamide 12b. In a similar way, starting from **11b**, compound **12b** was obtained as a solid (1.18 g, 96.8%).

HPLC: 4.60 min. ^{1}H NMR (200 MHz, $CDCl_3$): δ 8.26–8.17 (m, 1H), 8.11 (s, 1H), 7.76–7.68 (m, 1H), 7.60–6.82 (m, 5H), 3.15 (s, 1H).

Both compounds were used for the following synthesis of **13a** and **13b** without further purification.

6*H*-Dibenzo[*b*,*f*][1,5,2]dithiazepine 5,5-dioxide 13a. A solution of compound **12a** (1.52 g, 4.4 mmol) in 2-ethoxyethanol (60 mL) was treated with elemental copper (0.56 g, 8.8 mmol), heated at reflux and then treated with cuprous oxide (0.31 g, 2.2 mmol) and refluxed for 20 min. The hot bath was removed. The reaction mixture was cooled with a cold water bath and, after filtration by suction, the filtered solution was evaporated to give an oil that was treated with boiling ethyl acetate. The insoluble material was recovered by filtration, and was characterized as the dimer compound **15a** (see data below). The filtered solution was treated with hexane and the desired

product crystallized to give **13a** (0.926 g, 80%), mp 118–119 °C. HPLC: 3.67 min, >99% purity. ^{1}H NMR (600 MHz, DMSO-d_6): δ 10.78 (s, 1H), 7.92–7.88 (m, 1H), 7.67–7.64 (m, 1H), 7.61–7.56 (m, 1H), 7.53–7.44 (m, 2H), 7.37–7.33 (m, 1H), 7.25–7.20 (m, 2H). ESI$^-$ [M − H]$^-$ = m/z 262 HRMS: m/z 261.9996 ([$C_{12}H_9NO_2S_2$ − H]$^-$; calc. 261.9996).

11*H*,22*H*-5,10,16,21-Tetrathia-11,22-diazatetrabenzo[*a*,*d*,*h*,*k*]-cyclotetradecene 10,10,21,21-tetraoxide 15a. mp 380–382 °C decomp. (DMSO). HPLC: 5.16 min. ^{1}H NMR (600 MHz, DMSO-d_6): δ 9.58 (s, 2H), 7.97–7.93 (m, 2H), 7.70–7.66 (m, 2H), 7.58–7.55 (m, 2H), 7.43–7.36 (m, 4H), 6.97–6.92 (m, 2H), 6.89–6.84 (m, 2H), 5.76–5.72 (m, 2H). ESI$^+$ [M + H]$^+$ = m/z 527. HRMS: m/z 527.0213 ([$C_{24}H_{18}N_2O_4S_4$ + H]$^+$; calc. 527.0228).

8-Chloro-6*H*-dibenzo[*b*,*f*][1,5,2]dithiazepine 5,5-dioxide 13b. In a similar way as for **13a**, starting from compound **12b** (0.49 g, 1.3 mmol), **13b** was obtained as solid which was crystallized from hexane–ethyl acetate (0.75 g, 26%).

HPLC: 4.16 min, > 99% purity. ^{1}H NMR (600 MHz, DMSO-d_6): δ 11.03 (br s, 1H), 7.93–7.91 (m, 1H), 7.69–7.66 (m, 1H), 7.65–7.61 (m, 1H), 7.56–7.53 (m, 1H), 7.51 (d, J = 8.5 Hz, 1H), 7.28 (dd, J = 8.5, 2.3 Hz, 1H), 7.24 (d, J = 2.3 Hz, 1H). ESI$^-$ [M − H]$^-$ = m/z 296. HRMS: m/z 295.9612 ([$C_{12}H_8NO_2S_2Cl$ − H]$^-$; calc. 295.9607).

6*H*-Dibenzo[*b*,*f*][1,5,2]dithiazepine 5,5,11,11-tetraoxide 14a. A solution of compound **13a** (0.66 g, 2.5 mmol) in CH_2Cl_2 (40 mL) was treated, under stirring, with 3-chloroperbenzoic acid 77% (1.12 g, 5 mmol). The mixture was stirred at room temperature overnight and then it was diluted with CH_2Cl_2 (250 mL). The solution was washed with $NaHCO_3$ (5% aqueous solution, 100 mL) containing sodium thiosulfate (10% aqueous solution, 25 mL). Drying the organic phase with phase separator and removal of the solvent under reduced pressure gave **14a** (0.40 g, 55% yield), mp 229–230 °C decomp. (from ethyl acetate–hexane). HPLC: 3.16 min, 97.2% purity. ^{1}H NMR (600 MHz, DMSO-d_6): δ 11.71 (br s, 1H), 8.32–8.28 (m, 1H), 8.14–8.06 (m, 2H), 8.00–7.87 (m, 3H), 7.73–7.65 (m, 2H). ESI$^-$ [M − H$^-$] = m/z 294. HRMS: m/z 293.9898 ([$C_{12}H_9NO_4S_2$ − H]$^-$; calc. 293.9895).

8-Chloro-6*H*-dibenzo[*b*,*f*][1,5,2]dithiazepine 5,5,11,11-tetraoxide 14b. In a similar way, starting from compound **13b** (0.36 g, 1.2 mmol), **14b** was obtained as a crude solid which was purified in boiling water. The insoluble substance was filtered from the hot suspension, obtaining the pure product **14b** (0.33 g, 83%).

HPLC: 3.63 min, >99% purity. ^{1}H NMR (600 MHz, DMSO-d_6): δ 11.86 (br s, 1H), 8.32–8.27 (m, 1H), 8.13 (d, J = 8.5 Hz, 1H), 8.10–8.07 (m, 1H), 8.01–7.97 (m, 1H), 7.93–7.90 (m, 1H), 7.79 (d, J = 8.5 Hz, 1H), 7.76 (dd, J = 8.5, 1.9 Hz, 1H). ESI$^-$ [M − H$^-$] = m/z 328. HRMS: m/z 327.9502 ([$C_{12}H_8NO_4S_2Cl$ − H]$^-$; calc. 327.9505).

Crystal data and refinement

Intensity data were collected on an Oxford Diffraction Xcalibur diffractometer equipped with a CCD area detector, using Mo-Kα radiation (0.71073 Å) monochromated with a graphite prism for compounds **4a**, **8b**, **13a**, **14a**, **15a**·Me_2SO, while for compound **5b**·Me_2SO, Cu-Kα radiation (1.54018 Å) was used. All the data, except for compound **15a**·Me_2SO (T = 150 K), were collected at room temperature. Data were collected through the program CrysAlis CCD[29] and the reduction was carried on with the program CrysAlis RED.[30] Absorption correction was performed with the program ABSPACK in CrysAlis RED. Structures were solved with the direct methods of the SIR97[31] package and refined by full-matrix least squares against F^2 with the program SHELX97.[32]

Geometrical calculations were performed by PARST97[33] and molecular plots were produced by the program ORTEP3.[34]

In all the six structures all the non-hydrogen atoms were refined anisotropically. Concerning the hydrogen atoms in compounds **4a**, **8b** and **13a** they were all found in the Fourier

Table 6 Crystallographic data and refinement parameters for **4a**, **8b**, **13a**, **14a**, **5b**·Me_2SO and **15a**·Me_2SO (refinement method: full-matrix least-squares on F^2)

	4a	**8b**	**13a**	**14a**	**5b**·Me_2SO	**15a**·Me_2SO
Chemical formula	$C_{12}H_9NO_3S$	$C_{12}H_9N_2O_2SBr$	$C_{12}H_9NO_2S_2$	$C_{12}H_9NO_4S_2$	$C_{26}H_{22}N_2O_7S_3Cl_2$	$C_{26}H_{24}N_2O_5S_5$
M	247.26	325.18	263.32	295.32	641.54	604.77
T/K	298	298	298	298	298	150
λ/Å	0.71073	0.71073	0.71073	0.71073	1.54018	0.71073
Crystal system	Orthorhombic	Triclinic	Monoclinic	Triclinic	Monoclinic	Triclinic
Space group	$Pna2_1$	$P\bar{1}$	$P2_1/a$	$P\bar{1}$	$P2_1/a$	$P\bar{1}$
a/Å	8.342(1)	7.333(2)	7.1412(5)	8.050(3)	8.4934(4)	9.261(2)
b/Å	9.678(2)	8.131(3)	22.255(2)	8.123(3)	40.567(2)112.706(6)	10.064(4)
c/Å	13.675(2)	10.314(2)	7.9556(8)	11.287(6)	8.9646(7)	15.947(5)
α/°		97.41(2)		101.816(9)		99.54(3)
β/°		90.15(2)	109.175(8)	97.338(9)		90.98(2)
γ/°		91.61(2)		119.11(2)		112.46(3)
V/Å^3	1104.0(3)	609.5(3)	1194.2(2)	608.5(5)	2849.4(3)	1349.3(7)
Z, D_c/g cm^{-3}	4, 1.488	2, 1.772	4, 1.465	2, 1.612	4, 1.495	2, 1.489
μ/mm^{-1}	0.287	3.537	0.433	0.446	4.522	0.471
Reflections collected/unique	6149/2174	2963/2394	8323/2569	3621/1709	11 997/4254	8850/4149
Data/parameters	2174/190	2394/199	2569/190	1709/176	4254/371	4149/343
Final R indices	$R1$ = 0.0354	$R1$ = 0.0441	$R1$ = 0.0428	$R1$ = 0.0567	$R1$ = 0.0598	$R1$ = 0.0883
[$I > 2\sigma(I)$]	$wR2$ = 0.0629	$wR2$ = 0.1141	$wR2$ = 0.0795	$wR2$ = 0.1042	$wR2$ = 0.1633	$wR2$ = 0.2886
R indices	$R1$ = 0.0712	$R1$ = 0.0690	$R1$ = 0.0972	$R1$ = 0.1564	$R1$ = 0.0820	$R1$ = 0.1040
(all data)	$wR2$ = 0.0698	$wR2$ = 0.1309	$wR2$ = 0.1000	$wR2$ = 0.1189	$wR2$ = 0.1715	$wR2$ = 0.2933

synthesis and refined isotropically. In compounds **14a** and **5b**·Me_2SO the hydrogen atoms bonded to the nitrogen atoms were found in the Fourier synthesis and refined isotropically, all the other hydrogens were introduced in calculated position and refined in agreement with the coordinates of the atoms to which they are bound.

Finally in compound **15a**·Me_2SO all the hydrogen atoms were introduced in calculated positions and refined in agreement with the coordinates of the atoms to which they are bound. Fig. 4–9 report ORTEP3 views of the six structures.

Crystallographic data and refinement parameters for the six structures are reported in Table 6.

Computational study

The GAUSSIAN03 (Revision B.05)[35] package implemented on a personal computer was used for all the computational studies concerning the monomers (see Fig. 3, Scheme 8 and ref. 28). In all cases the level of theory was HF-SCF, the basis set was 6-311 + G(d,p).[36] The Berny algorithm[37] was used for the optimization procedure. The reliability of the stationary points was assessed by the evaluation of the vibrational frequencies. NBO analyses were performed using the NBO 5.0 program.[26] Given that the oxo (**4a**), amine (**8b**) and sulfur derivatives (**13a** and **14a**) show in the solid state three distinct overall geometries, namely **I**, **II** and **III** (see Scheme 8 and the X-ray structure discussion in the *Solid state characterization results* paragraph), for each modelled molecule sketched in Fig. 3, three starting geometries were considered and fully optimized (**4a-I**/**4a-III**; **8a-I**/**8a-III**; **13a-I**/**13a-III**; **14a-I**/**14a-III**). Tables 1–4 list the most interesting geometrical optimized parameters, Table 5 reports the relative energy contents of each optimized species.

References

1 (*a*) B. E. Evans, K. E. Rittle, M. G. Bock, R. M. DiPardo, R. M. Freidinger, W. L. Whittle, G. F. Lundell, D. F. Veber, P. S. Anderson, R. S. L. Chang, V. J. Lotti, D. J. Cerino, T. B. Chen, P. J. Kling, K. A. Kunkel, J. P. Springer and J. Hirshfield, *J. Med. Chem.*, 1988, **31**, 2235; (*b*) A. A. Patchett and R. P. Nargund, *Annu. Rep. Med. Chem.*, 2000, **35**, 289.

2 V. Fedi, A. Guidi and M. Altamura, *Mini-Rev. Med. Chem.*, 2008, **8**, 1464.

3 M. Paris, M. Porcelloni, M. Binaschi and D. Fattori, *J. Med. Chem.*, 2008, **51**, 1505.

4 (*a*) D. Giannotti, G. Viti, P. Sbraci, V. Pestellini, G. Volterra, F. Borsini, A. Lecci, A. Meli, P. Dapporto and P. Paoli, *J. Med. Chem.*, 1991, **34**, 1356; (*b*) D. Giannotti, G. Viti, R. Nannicini, V. Pestellini and D. Bellarosa, *Bioorg. Med. Chem. Lett.*, 1995, **5**, 1461; (*c*) M. Altamura, P. Dapporto, A. Guidi, N. J. S. Harmat, L. Jierry, E. Libralesso, P. Paoli and P. Rossi, *New J. Chem.*, 2008, **32**, 1617.

5 E. J. Warawa, B. M. Migler, C. J. Ohnmacht, A. L. Needles, G. C. Gatos, F. M. McLaren, C. L. Nelson and K. M. Kirkland, *J. Med. Chem.*, 2001, **44**, 372.

6 (*a*) K. Hiroshi and M. Mitsuru, *Jap. Pat.*, JP 45015983, 1970; (*b*) E. Enders, F. Muth and H. Herlinger, *GB Pat.*, GB 1013046, 1963; (*c*) K. Nagarajan, V. Ranga, A. Venkarlu and R. K. Shah, *Indian J. Chem.*, 1974, **12**, 252.

7 (*a*) J. Jabicky, *The Chemistry of Amides*, Interscience, London, 1970; (*b*) Y. Hiroshi, U. Norihiro, N. Jun, S. Hiroyuki, K. Yoshihiko, K. Nozomu, Y. Kentaro, A. Makoto and W. Tatsuo, *J. Med. Chem.*, 1992, **35**, 2496.

8 S. Senger, C. Chan, M. A. Convery, J. A. Hubbard, G. P. Shah, N. S. Watson and R. J. Young, *Bioorg. Med. Chem. Lett.*, 2007, **17**, 2931.

9 (*a*) A. Weber and J. Frossard, *Ann. Pharm. Fr.*, 1966, **6**, 445; (*b*) N. Lebegue, S. Gallet, N. Flouquet, P. Carato, S. Giraudet and P. Berthelot, *Heterocycles*, 2004, **63**, 2457; (*c*) N. Lebegue, S. Gallet, N. Flouquet, P. Carato, B. Pfeiffer, P. Renard, S. Léonce, A. Pierré, P. Chavatte and P. Berthelot, *J. Med. Chem.*, 2005, **48**, 7363.

10 R. A. Abramovitch, C. I. Azogu, I. T. McMaster and D. P. Vanderpool, *J. Org. Chem.*, 1978, **43**, 1218.

11 K. Kunz, U. Scholz and D. Ganzer, *Synlett*, 2003, 2428.

12 (*a*) M. Carril, R. SanMartin, F. Churruca, I. Tellitu and E. Dominguez, *Org. Lett.*, 2005, **7**, 4787; (*b*) M. Carril, R. SanMartin, E. Dominguez and I. Tellitu, *Tetrahedron*, 2007, **63**, 690.

13 N. Hucher, B. Decroix and A. Daich, *J. Org. Chem.*, 2001, **66**, 4695.

14 F. H. Allen, *Acta Crystallogr., Sect. B: Struct. Sci.*, 2002, **58**, 380.

15 (*a*) H. Bock, N. Nagel and C. Naether, *Z. Naturforsch., Teil B*, 1998, **53**, 1389; (*b*) A. Parkin, A. Collins, C. J. Gilmore and C. C. Wilson, *Acta Crystallogr., Sect. B: Struct. Sci.*, 2008, **64**, 66.

16 (*a*) R. D. Bindal, J. T. Golab and J. A. Katzenellenbogen, *J. Am. Chem. Soc.*, 1990, **112**, 7861; (*b*) J. B. Nicholas, R. Vance, E. Martin, B. J. Burke and A. J. Hopfinger, *J. Phys. Chem.*, 1991, **95**, 9803; (*c*) J. Heyd, W. Thiel and W. Weber, *J. Mol. Struct. (THEOCHEM)*, 1997, **391**, 125; (*d*) G. Liang, J. P. Bays and J. P. Bowen, *J. Mol. Struct. (THEOCHEM)*, 1997, **401**, 165.

17 T. C. Higgs, A. Parkin, S. Parsons and P. A. Tasker, *Acta Crystallogr., Sect. E: Struct. Rep. Online*, 2002, **58**, o523.

18 K. B. Wiberg, *Advances in Molecular Modeling*, ed. D. Liotta, Jai Press, London, 1988.

19 K. A. Brameld, B. Kuhn, D. C. Reuter and M. Stahl, *J. Chem. Inf. Model.*, 2008, **48**, 1.

20 M. C. Menziani, M. Cocchi and P. G. De Benedetti, *J. Mol. Struct. (THEOCHEM)*, 1992, **256**, 217.

21 V. Petrov, V. Petrova, G. V. Girichev, H. Oberhammer, N. I. Giricheva and S. Ivanov, *J. Org. Chem.*, 2006, **71**, 2952.

22 V. M. Petrov, G. V. Girichev, H. Oberhammer, V. N. Petrova, N. I. Giricheva, A. V. Bardina and S. N. Ivanov, *J. Phys. Chem. A*, 2008, **112**, 2969.

23 W. L. Duax, C. M. Weeks and D. C. Rohrer, *Top. Stereochem.*, 1976, **9**, 271.

24 V. Bertolasi, V. Ferretti, G. Gilli and P. A. Borea, *Cryst. Struct. Commun.*, 1982, **11**, 1481.

25 C. A. Hunter and J. K. M. Sanders, *J. Am. Chem. Soc.*, 1990, **112**, 5525.

26 E. D. Glendening, J. K. Badenhoop, A. E. Reed, J. E. Carpenter, J. A. Bohmann, C. M. Morales and F. Weinhold, NBO 5.0., Theoretical Chemical Institute, University of Wisconsin, Madison, WI, 2001.

27 A. Bondi, *J. Phys. Chem.*, 1964, **68**, 441.

28 To assess the role of steric effects in driving the tricyclic arrangement, geometry optimizations were performed of two further molecular models having Z = CH_2 and $C(CH_3)_2$ (CH_2-**I**, CH_2-**III**, $C(CH_3)_2$-**I** and $C(CH_3)_2$-**III**). Assuming that the steric hindrance exerted by the methylene group is negligible when Z = CH_2, the electronic factors should prevail in driving the molecular geometry, while in the bulkier derivative (Z = $C(CH_3)_2$) the steric repulsions should play the leading role. As a matter of fact CH_2-**I** is more stable than CH_2-**III**. As for the bulkier derivative (Z = $C(CH_3)_2$), the steric effects appear important as provided by the re-arrangement of the both the **I** and **III** geometries during the minimization processes, which indicate the $C(CH_3)_2$-**III** as the most stable conformer. Finally the electronic picture of each model, provided by the NBO analysis, is in keeping with that already presented and discussed.

29 CrysAlis CCD, Oxford Diffraction Ltd., Version 1.171.29.2 (release 20.01.2006 CrysAlis171.NET).

30 CrysAlis RED, Oxford Diffraction Ltd., Version 1.171.29.2 (release 20.01.2006 CrysAlis171. NET).

31 A. Altomare, G. L. Cascarano, C. Giacovazzo, A. Guagliardi, A. G. Moliterni, M. C. Burla, G. Polidori, M. Camalli and R. Spagna, *J. Appl. Crystallogr.*, 1999, **32**, 115.

32 G. M. Sheldrick, SHELX 97, University of Göttingen, Germany, 1997.
33 M. Nardelli, *J. Appl. Crystallogr*., 1995, **28**, 659.
34 L. J. Farrugia, *J. Appl. Crystallogr*., 1997, **30**, 565.
35 M. J. Frisch, G. W. Trucks, H. B. Schlegel, G. E. Scuseria, M. A. Robb, J. R. Cheeseman, J. A. Montgomery, Jr., T. Vreven, K. N. Kudin, J. C. Burant, J. M. Millam, S. S. Iyengar, J. Tomasi, V. Barone, B. Mennucci, M. Cossi, G. Scalmani, N. Rega, G. A. Petersson, H. Nakatsuji, M. Hada, M. Ehara, K. Toyota, R. Fukuda, J. Hasegawa, M. Ishida, T. Nakajima, Y. Honda, O. Kitao, H. Nakai, M. Klene, X. Li, J. E. Knox, H. P. Hratchian, J. B. Cross, V. Bakken, C. Adamo, J. Jaramillo, R. Gomperts, R. E. Stratmann, O. Yazyev, A. J. Austin, R. Cammi, C. Pomelli, J. Ochterski, P. Y. Ayala, K. Morokuma, G. A. Voth, P. Salvador, J. J. Dannenberg, V. G. Zakrzewski, S. Dapprich, A. D. Daniels, M. C. Strain, O. Farkas, D. K. Malick, A. D. Rabuck, K. Raghavachari, J. B. Foresman, J. V. Ortiz, Q. Cui, A. G. Baboul, S. Clifford, J. Cioslowski, B. B. Stefanov, G. Liu, A. Liashenko, P. Piskorz, I. Komaromi, R. L. Martin, D. J. Fox, T. Keith, M. A. Al-Laham, C. Y. Peng, A. Nanayakkara, M. Challacombe, P. M. W. Gill, B. G. Johnson, W. Chen, M. W. Wong, C. Gonzalez and J. A. Pople, *GAUSSIAN 03 (Revision B.5)*, Gaussian, Inc., Wallingford, CT, 2004.
36 T. Clark, J. Chandrasekhar, G. W. Spitznagel and P. v. R. Schleyer, *J. Comput. Chem*., 1983, **4**, 294.
37 C. Peng, P. Y. Ayala, H. B. Schlegel and M. J. Frisch, *J. Comput. Chem*., 1996, **17**, 49.